

SUPPLEMENTARY MATERIAL

Supplementary Table 1: Patient and aneurysm characteristics of the training and testing datasets.

Characteristics		Training Dataset	Testing Dataset
Population	US	546	49
	EU	84	-
	SA	3	-
	FIN	38	14
	JAP	93	-
Patient	Age	56.4 [12-90] y	53.3 [25-69] y
	Sex	F=570 (75%), M=194 (25%)	F=49 (78%), M=14 (22%)
	Multiplicity	M=344 (45%), S=420 (55%)	M=23 (37%), S=40 (63%)
	Total	764	63
Aneurysm	Size	4.1 [1.1-6.9] mm	4.4 [1.3-6.9] mm
	Rupture	R=197 (18%), U=882 (82%)	R=14 (14%), U=88 (86%)
	Total	1079	102

Rupture: R= ruptured, U= unruptured. Sex: F=female, M=male. Multiplicity: M=multiple, S=single.

Supplementary Table 2: Patient and aneurysm characteristics associated with aneurysm rupture.

Characteristics	Values	Ruptured Aneurysms	Unruptured Aneurysms	p-value	Adjusted p-value
Patient characteristics					
Age	Age	53.9 ± 14.1 y	57.3 ± 13.7 y	0.003*	0.003*
Sex	Female	133 (23%)	437 (77%)	0.01*	0.01*
	Male	63 (32%)	131 (68%)		
Population	US	156 (29%)	390 (71%)	<0.001*	<0.001*
	EU	19 (23%)	65 (77%)		
	SA	0 (0%)	3 (100%)		
	FIN	16 (42%)	22 (58%)		
	JAP	5 (5%)	88 (95%)		
Aneurysm characteristics					
Multiplicity	Multiple	47 (7%)	612 (93%)	<0.001*	<0.001*
	Single	150 (36%)	270 (64%)		
Morphology	Bifurcation	157 (23%)	521 (77%)	<0.001*	<0.001*
	Lateral	40 (10%)	361 (90%)		
Location	ACA	13 (25%)	38 (75%)	<0.001*	<0.001*
	ACOM	51 (42%)	70 (58%)		
	BA	7 (19%)	30 (81%)		
	ICA	41 (9%)	421 (91%)		
	MCA	47 (19%)	204 (81%)		
	PCOM	35 (14%)	116 (86%)		
	PICA	3 (50%)	3 (50%)		

Statistically significant p-values are indicated with a “*”.

ACA, anterior cerebral artery; ACOM, anterior communicating artery; BA, basilar artery; ICA, internal carotid artery; MCA, middle cerebral artery; PCOM, posterior communicating artery; PICA, posterior inferior cerebellar artery.

Supplementary Table 3: Hemodynamic and geometric characteristics associated with rupture in small (<7mm) regularly shaped aneurysms.

Characteristic	Variable	Ruptured Aneurysms	Unruptured Aneurysms	p-value	Adjusted p-value
		Mean \pm SD	Mean \pm SD		
Hemodynamics					
Inflow jet	Q (ml/s)	0.35 \pm 0.35	0.30 \pm 0.33	0.01*	0.02*
	ICI	0.39 \pm 0.39	0.33 \pm 0.39	0.002*	0.002*
Flow pattern	VE (cm/s)	9.29 \pm 8.59	8.48 \pm 6.37	0.80	0.82
	VD	1065 \pm 1628	1041 \pm 1483	0.72	0.78
	corelen (mm)	6.93 \pm 5.99	4.35 \pm 5.33	<0.001*	<0.001*
	podent	0.15 \pm 0.11	0.13 \pm 0.11	<0.001*	<0.001*
Wall shear stress pattern	WSSmax (dyn/cm ²)	342 \pm 142	185 \pm 153	<0.001*	<0.001*
	WSSmean (dyn/cm ²)	25.4 \pm 35.6	22.1 \pm 19.8	0.82	0.82
	MaxWSSnorm	6.16 \pm 11.7	4.89 \pm 3.08	0.002*	0.003*
	WSSnorm	0.51 \pm 0.36	0.57 \pm 0.34	0.01*	0.02*
	LSA (%)	48.5 \pm 33.4	48.7 \pm 33.1	0.69	0.78
	SCI	3.63 \pm 3.39	2.79 \pm 2.98	<0.001*	<0.001*
	OSI _{max}	0.24 \pm 0.11	0.19 \pm 0.12	<0.001*	<0.001*
	OSI _{mean}	0.012 \pm 0.011	0.009 \pm 0.013	<0.001*	<0.001*
	nCrPoints	1.66 \pm 0.98	1.05 \pm 0.89	<0.001*	<0.001*
Geometry					
Size	Asize (mm)	4.6 \pm 1.3	3.9 \pm 1.4	<0.001*	<0.001*
	Nsize (mm)	3.3 \pm 0.9	3.4 \pm 1.2	0.55	0.66
	SR	1.59 \pm 0.66	1.18 \pm 0.51	<0.001*	<0.001*
	GAA (cm ⁻¹)	22.1 \pm 16.7	29.4 \pm 25.7	<0.001*	<0.001*
Elongation	AR	0.93 \pm 0.48	0.66 \pm 0.36	<0.001*	<0.001*
	VOR (mm)	2.98 \pm 2.65	1.86 \pm 1.86	<0.001*	<0.001*
	BF	1.10 \pm 0.29	0.99 \pm 0.20	<0.001*	<0.001*
Shape distortion	NSI	0.21 \pm 0.05	0.19 \pm 0.05	<0.001*	<0.001*
	CR	0.76 \pm 0.12	0.72 \pm 0.13	<0.001*	<0.001*
Irregularity	UI	0.24 \pm 0.12	0.28 \pm 0.13	<0.001*	<0.001*

Significant differences (95% confidence, p<0.05 in two-sided tests) are marked with a “*”. The ‘Adjusted p-value’ column lists the p-values after adjustment for multiple testing using the Benjamini & Hochberg method.

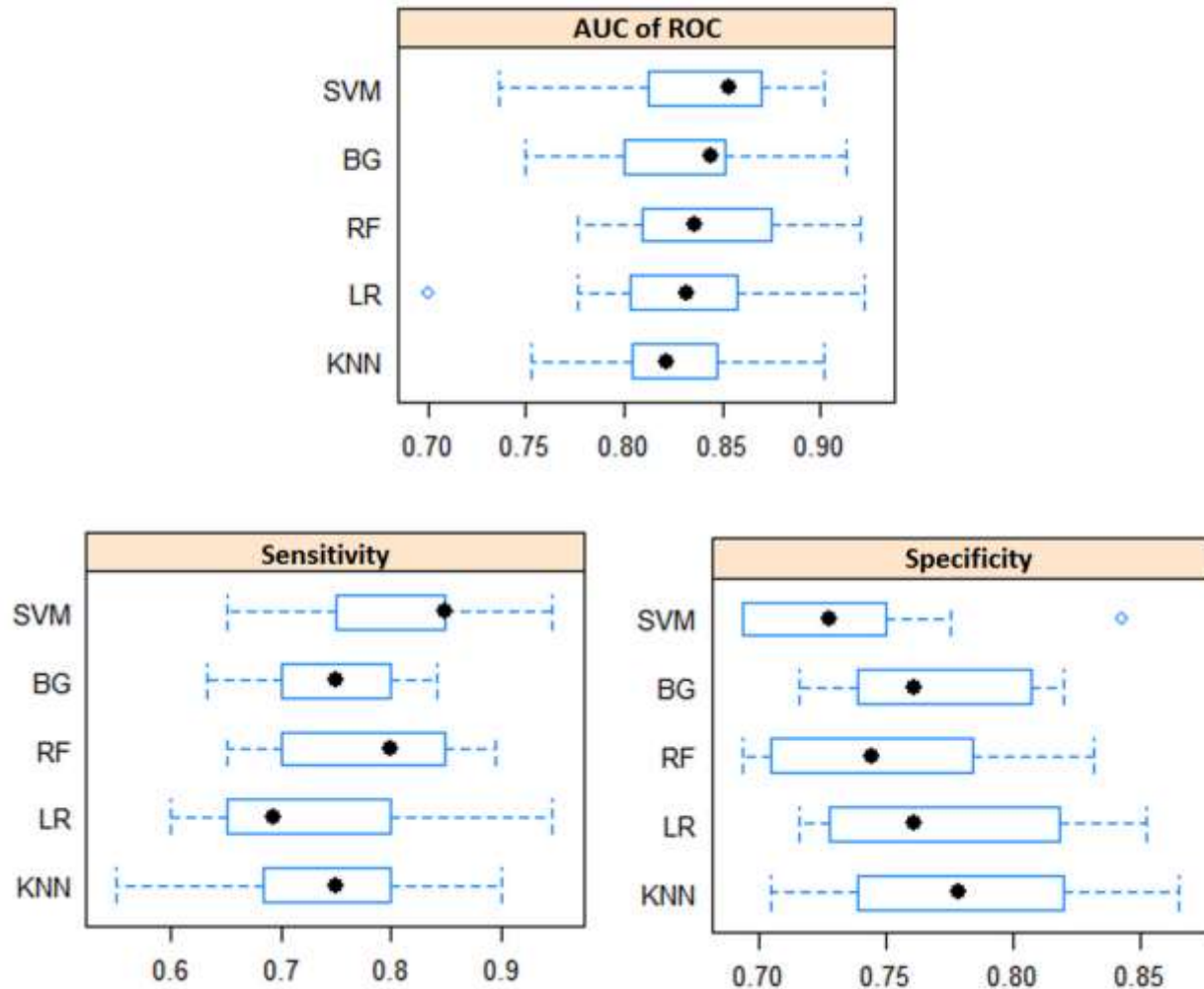
Supplementary Table 4: Variables considered for rupture predictive modeling of small regularly shaped aneurysms from four different domains.

Domain	Variable	Meaning	Retained
Patient	Age	Patient age (years)	No
	Sex	Patient sex (F/M)	No
	Population	Patient population (US, EU, SA, FIN, JAP)	No
Aneurysm	Location	Aneurysm location (ACA,ACOM,BA,ICA,MCA,PCOM,PICA)	Yes
	Morphology	Aneurysm morphology (lateral/bifurcation)	Yes
	Multiplicity	Aneurysm multiplicity (single/multiple)	Yes
Hemodynamics	Q	Mean aneurysm inflow rate (ml/s)	No
	ICI	Inflow concentration index	No
	VE	Mean aneurysm velocity (cm/s)	No
	VD	Mean aneurysm viscous dissipation	No
	corelen	Total vortex core-line length	Yes
	podent	Proper orthogonal decomposition entropy	No
	WSSmax	Maximum wall shear stress	Yes
	WSSmean	Time averaged mean wall shear stress	No
	MWSSnorm	Max normalized WSS (over vessel WSS)	No
	WSSnorm	Mean normalized WSS	No
	LSA	Percent of aneurysm area under low WSS	No
	SCI	Shear concentration index	No
	OSI _{max}	Maximum oscillatory shear index	Yes
	OSI _{mean}	Mean oscillatory shear index	Yes
	nCrPoints	Time-averaged number of critical points in WSS field	Yes
Geometry	Asize	Aneurysm maximum size	Yes
	Nsize	Neck maximum size	No
	SR	Size ratio	Yes
	GAA	Gaussian curvature	No
	AR	Aspect ratio	Yes
	VOR	Volume to ostium ratio	Yes
	BF	Bottleneck factor	Yes
	NSI	Non-sphericity index	Yes
	CR	Convexity ratio	No
	UI	Undulation index	No

Supplementary Table 5: Pair-wise statistical significance scores between predictive models for different evaluation metrics.

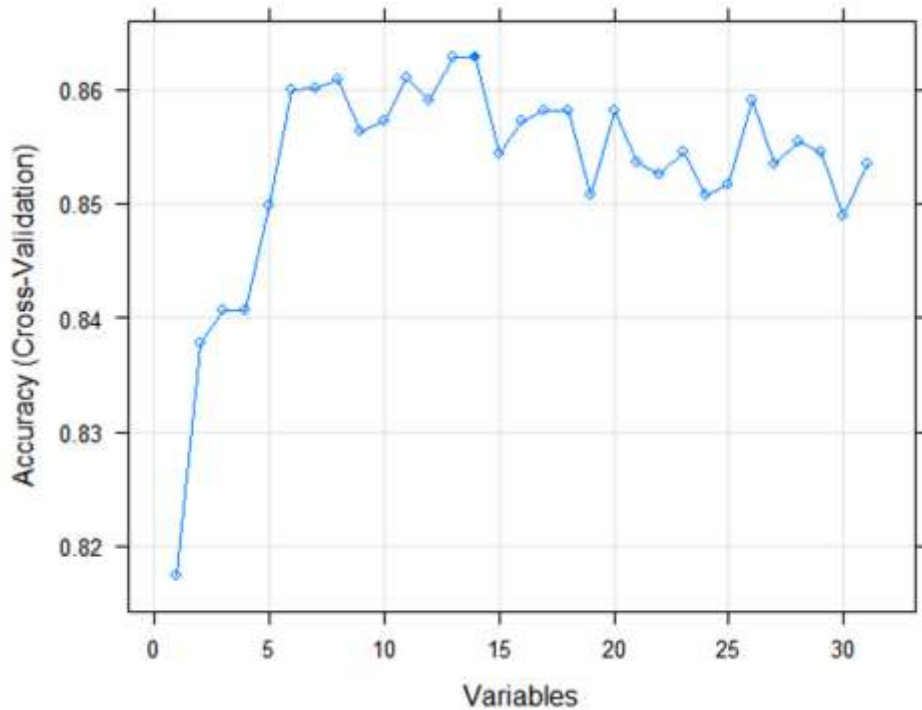
Comparison	AUC (p-value)	Sensitivity (p-value)	Specificity (p-value)
BG vs. RF	0.49	0.21	0.25
BG vs. SVM	0.17	0.003*	0.03*
BG vs. KNN	0.16	0.76	0.19
BG vs. LR	0.48	0.38	0.47
RF vs. SVM	0.38	0.13	0.22
RF vs. KNN	0.08	0.26	0.14
RF vs. LR	0.17	0.03*	0.14
SVM vs. KNN	0.15	0.03*	0.01*
SVM vs. LR	0.02*	0.006*	0.02*
KNN vs. LR	0.86	0.64	0.73

The differences were computed using a t-test to evaluate the null hypothesis that there is no difference between models.

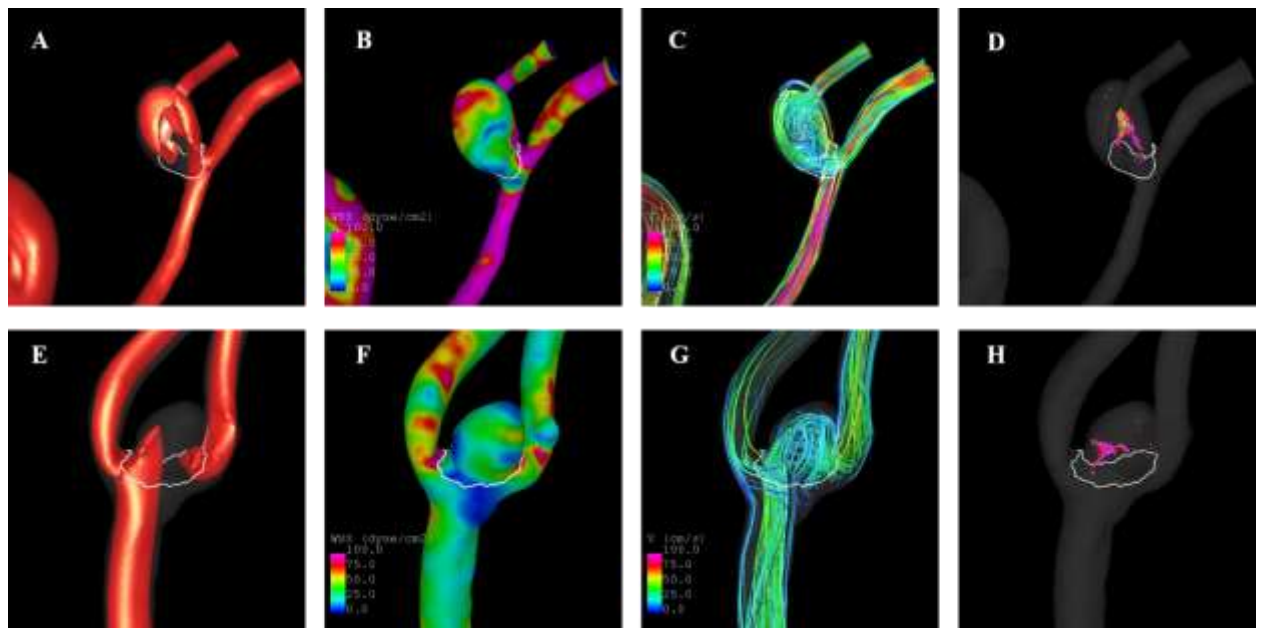


Supplementary Figure 1: Box-whisker plot showing sensitivity, specificity, and AUC of the ROC for different models during the resampling procedure. The boxes are ordered from highest to lowest mean AUC, sensitivity (TPR: ratio of true to all positives), and specificity (1-FPR, ratio of false positives to all negatives). The spread of these measures for each algorithm corresponds to repeated evaluations during the 10-fold cross-validation process.

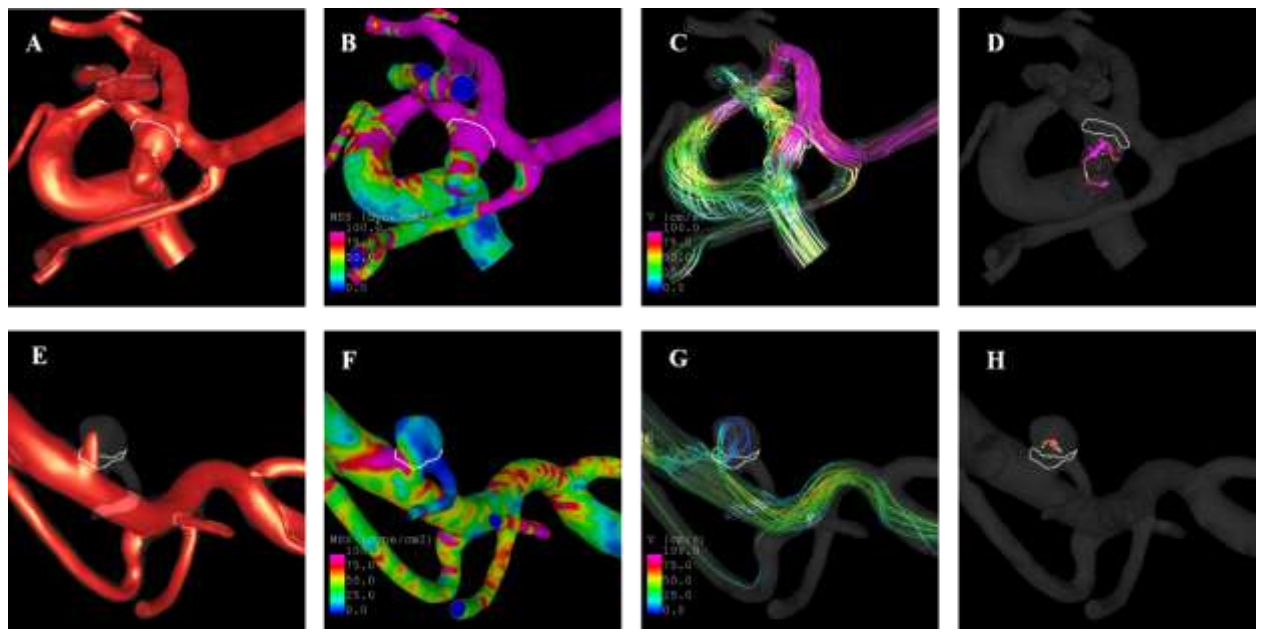
Accuracy of the Model Based on the Number of Variables



Supplementary Figure 2: Accuracy of machine learning models with different number of variables (in decreasing order of importance) during the 10-fold cross-validation process.



Supplementary Figure 3: Examples of hemodynamics (at peak systole) for small (<7mm) and regularly shaped ruptured and unruptured anterior communicating artery (ACOM) aneurysms correctly classified with the SVM model. Top panel – ruptured ACOM aneurysm: a) inflow jet (iso-velocity surface), b) wall shear stress (WSS) magnitude, c) flow pattern (streamlines), d) vortex corelines. Bottom panel – representative unruptured ACOM aneurysm: e) inflow jet, f) WSS magnitude, g) flow pattern, and h) vortex corelines.



Supplementary Figure 4: Examples of hemodynamics (at peak systole) for small (<7mm) and regularly shaped ruptured and unruptured middle cerebral artery (MCA) aneurysms correctly classified with the SVM model. Top panel – ruptured MCA aneurysm: a) inflow jet (iso-velocity surface), b) wall shear stress (WSS) magnitude, c) flow pattern (streamlines), d) vortex corelines. Bottom panel – representative unruptured MCA aneurysm: e) inflow jet, f) WSS magnitude, g) flow pattern, and h) vortex corelines.